chemistry

MDPI

Article

Synthesis, Dynamic NMR Characterization, and XRD Study of 2,4-Difluorobenzoyl-Substituted Piperazines

Martin Köckerling [1] and Constantin Mamat [2,3,*]

[1] Institut für Chemie—Festkörperchemie, Universität Rostock, Albert-Einstein-Straße 3a, D-18059 Rostock, Germany; martin.koeckerling@uni-rostock.de
[2] Helmholtz-Zentrum Dresden-Rossendorf, Institut für Radiopharmazeutische Krebsforschung, Bautzner Landstraße 400, D-01328 Dresden, Germany
[3] Fakultät Chemie und Lebensmittelchemie, Technische Universität Dresden, D-01062 Dresden, Germany
* Correspondence: c.mamat@hzdr.de

Abstract

Five different 2,4-difluorobenzamide derivatives were synthesized and fully characterized by $^{1}H/^{13}C/^{19}F/2D$ NMR spectroscopy using DMSO-d_6 as solvent and MS. All compounds occur as rotation conformers resulting from the partial amide double bond with a solvent-dependent coalescence point. Temperature-dependent ^{1}H NMR techniques, as well as EXSY, were applied to determine the rate constants of exchange, and the resulting activation energy barriers were calculated. Regarding the *N*,*N*-diacylated piperazine, both conformers (*syn* and *anti*) were found in solution, whereas only the *anti*-conformer was found in the crystals. This result was verified by an XRD analysis. Single crystals of *N*,*N*-bis(2,4-difluorobenzoyl)piperazine **3b** (monoclinic, space group $P2_1/c$, a = 7.2687(3), b = 17.2658(8), c = 6.9738(3) Å, β = 115.393(2)°, V = 790.65(6) Å^3, Z = 4, D_{obs} = 1.530 g/cm^3) were obtained from a saturated chloroform solution.

Keywords: rotational barrier; coalescence; dynamic NMR; labeling

check for updates

Academic Editor: Angelo Frongia

Received: 28 August 2025
Revised: 29 September 2025
Accepted: 30 September 2025
Published: 3 October 2025

Citation: Köckerling, M.; Mamat, C. Synthesis, Dynamic NMR Characterization, and XRD Study of 2,4-Difluorobenzoyl-Substituted Piperazines. *Chemistry* **2025**, *7*, 162. https://doi.org/10.3390/chemistry7050162

Copyright: © 2025 by the authors. Licensee MDPI, Basel, Switzerland. This article is an open access article distributed under the terms and conditions of the Creative Commons Attribution (CC BY) license (https://creativecommons.org/licenses/by/4.0/).

1. Introduction

Piperazines belong to saturated six-membered heterocyclic compounds containing two nitrogen atoms [1]. This scaffold has been integrated as a fundamental structural element into bioactive and pharmacologically relevant compounds [2–5]. *N*- and *N*,*N*-functionalized piperazine derivatives are used as intermediates in organic reactions [6,7] or for polymerization processes, ref. [8] as ligands in coordination chemistry [9–11] or as a scaffold for peptide syntheses and modifications [12,13]. Piperazines are also in use for the introduction of fluorescent dyes [14,15] or for the preparation of radiolabeled compounds [16–20]. They serve as skeletons in pesticides, pharmaceuticals [21–23], and other drugs [24–26] or basic scaffolds in medicinal chemistry [27–29]. Furthermore, the *N*,*N*-substituted benzamide scaffold is found in various natural products and drugs, such as in Ampakines [30,31].

Especially *N*-acylated piperazines containing a fluorobenzoyl or difluorobenzoyl group are of interest (Figure 1), as they function as serotonin 5-HT_{2A} receptor antagonists [32], cardiotonic agents [33], adenosine A_{2A} receptor antagonists [34], radiosensitizers for tumor therapy [35], or as a kinase inhibitor for Jun-kinase [36]. The comprehension of the conformational behavior of such functionalized piperazines is mandatory not only to explain biological and/or pharmacological effects, but also for applications in material sciences.

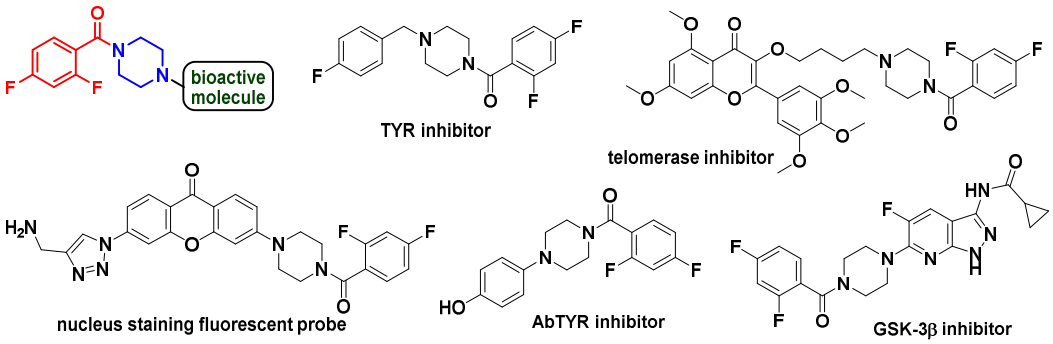

Figure 1. 2,4-Difluorobenzoylpiperazine moiety present in selected different biologically and pharmacologically active compounds such as TYR inhibitor [37], telomerase inhibitor [38], fluorescent probe for nucleus staining [39], AbTYR inhibitor [40] and GSK-3β inhibitor [41].

Secondary and tertiary *N*-acylated piperazines, in general, and especially *N*-benzoylated piperazines, exhibit a more complex conformational behavior due to the hindered rotation of the C–N amide bond. This phenomenon in amides is well known and has far-reaching implications for peptide and protein folding [42]. Additionally, the conformation of the piperazine ring itself has to be considered. However, NMR properties of such benzamides were only rarely studied in the past. *N*,*N*-dimethyl and *N*,*N*-diethyl benzamides represent the best characterized compounds [43–46]. The NMR behavior of selected benzoylpiperazines [47], which were also used as prosthetic groups for ^{18}F-radiolabeling [19], has been investigated. To expand the scope and to obtain a deeper insight into the conformational behavior of *N*- and *N*,*N*-substituted piperazines, two 2,4-difluorobenzoyl-containing derivatives were prepared and fully characterized in terms of their particular NMR behavior and compared with three *N*,*N*-disubstituted amides.

2. Materials and Methods

2.1. General

The starting materials were purchased from commercial suppliers and used without further purification unless otherwise specified. Anhydrous THF was purchased from Acros Organics. Mass spectrometric (MS) data was obtained on a mass spectrometer (expression CMS, Advion Interchim, Montluçon, France) by electrospray ionization (ESI). The melting points were determined on a Galen III melting point apparatus (Cambridge Instruments/Leica, Wetzlar, Germany) and are uncorrected. Chromatographic separations were performed using an automated flash chromatography system Selekt (Biotage, Uppsala, Sweden) with Sfär cartridges (Biotage, Uppsala, Sweden). TLC detections were performed using Merck (Darmstadt, Germany) Silica Gel 60 F_{254} sheets, respectively. TLCs were developed by visualization under UV light (λ = 254 nm).

2.2. VT-NMR Measurements

NMR spectra of all compounds were recorded on an Agilent DD2-400 MHz NMR spectrometer with a 5 mm ProbeOne probe. Deuterated solvents were purchased from deutero. Chemical shifts in the ^{1}H, ^{19}F, and ^{13}C spectra were reported in parts per million (ppm) using TMS as an internal standard for ^{1}H/^{13}C and $CFCl_3$ for ^{19}F spectra at 25 °C unless otherwise stated. Spectra were calibrated to their solvent signals. Dynamic NMR measurements were carried out in a temperature range of 253–393 K using the Agilent VT accessory with a digital temperature controller. The T_C was estimated from the NMR spectrum, which showed the collapse of the methylene signals from the piperazine moiety, and Δν values were extracted from the maximum split signals of the piperazine methylene protons, which remained unchanged with decreasing temperature. Values of the

exchange rate k_{exc} at T_C were calculated using equation $k_{exc} = \pi \cdot \Delta\nu / 2^{1/2}$ [48,49]. Values of the free activation energy, $\Delta G^{\ddagger}$, were obtained by solving the Eyring equation (1) for $\Delta G^{\ddagger}$ (2) [48,50]. in accordance with other studies on amide *cis*/*trans* isomerization, the transmission coefficient κ was assumed to be 1 [51].

$$k_{exc} = \frac{\kappa k_B T_C}{h} e^{-\frac{\Delta G^{\ddagger}}{RT_C}} \quad (1)$$

$$\Delta G^{\ddagger} = \ln\left(\frac{\kappa k_B T_C}{h k_{exc}}\right) RT_C \quad (2)$$

2.3. Single Crystal X-Ray Diffraction

Diffraction data was collected with a Bruker-Nonius Apex-II-diffractometer using graphite-monochromated MoK_α radiation (λ = 0.71073 Å). The diffraction measurement was performed at –150 °C. The unit cell dimensions were refined using the angular settings of 9936 reflections for **3b**. The structure was solved by direct methods and refined against F^2 using full-matrix least-squares with the program suites from G. M. Sheldrick [51,52]. All non-hydrogen atoms were refined anisotropically; all hydrogen atoms were placed on geometrically calculated positions and refined using riding models. CCDC 2238312 contains the supplementary crystallographic data for compound **3b**. This data can be obtained free of charge from The Cambridge Crystallographic Data Centre via www.ccdc.cam.ac.uk/data_request/cif (accessed on 27 August 2025).

2.4. Synthesis of *N*-(2,4-Difluorobenzoyl)piperazine (**3a**)

Piperazine (5 equiv.) was dissolved in absolute chloroform, 2,4-difluorobenzoyl chloride (1 equiv.) was added slowly at 0 °C, and the mixture was allowed to stir at 0 °C for another 5 h and at rt overnight. Afterwards, the solvent was removed and the crude mixture of products was purified via automated column chromatography, yielding *N*-(2,4-difluorobenzoyl)piperazine (**3a**) as a colorless solid in a yield of 66% and the *N*,*N*-diacylated compound **3b** (yield 10%). Mp > 260 °C; ^{1}H NMR (400 MHz, $CDCl_3$): δ = 2.92 (br. s, 2H, NCH_2), 3.03 (br. s, 2H, NCH_2), 3.39 (br. s, 2H, NCH_2), 3.85 (br. s, 2H, NCH_2), 6.85 (t, *J* = 9.0 Hz, 1H, ArH), 6.96 (t, *J* = 8.3 Hz, 1H, ArH), 7.40 (m, 1H, ArH) ppm; ^{13}C NMR (101 MHz, $CDCl_3$): δ = 42.4, 45.3, 45.8, 47.4 (4 × NCH_2), 104.4 (t, $J_{C,F}$ = 26 Hz, CH_{Ar}), 112.5 (dd, $J_{C,F}$ = 3 Hz, $J_{C,F}$ = 22 Hz, CH_{Ar}), 120.1 (dd, $J_{C,F}$ = 4 Hz, $J_{C,F}$ = 18 Hz, C_{Ar}), 130.8 (m, CH_{Ar}), 158.7 (dt, $J_{C,F}$ = 253 Hz, $J_{C,F}$ = 11 Hz, C_{Ar}), 164.0 (dt, $J_{C,F}$ = 251 Hz, $J_{C,F}$ = 12 Hz, C_{Ar}), 164.6 (C = O) ppm; MS (ESI+): *m*/*z* = 227 $[M+H]^+$.

2.5. Synthesis of *N*,*N*-Bis(2,4-difluorobenzoyl)piperazine (**3b**)

Piperazine (2 equiv.) was dissolved in absolute chloroform, 2,4-difluorobenzoyl chloride (1 equiv.) was added slowly at 0 °C, and the mixture was allowed to stir at rt overnight. Afterwards, the solvent was removed and the crude mixture of products was purified via automated column chromatography, yielding *N*,*N*-bis(2,4-difluorobenzoyl)piperazine (**3b**) in 44% yield as a colorless solid and the *N*-monoacylated compound **3a** (9% yield) from the one-pot reaction. Mp 245–247 °C; ^{1}H NMR (400 MHz, $CDCl_3$): δ = 3.34 (br. s, 2H, NCH_2), 2.44, 3.79, 3.89, 6.78–7.06 (m, 4H, ArH), 7.43 (dd, ^3J = 7.5 Hz, $^3J_{H,F}$ = 14.9 Hz, 2H, ArH) ppm; ^{13}C NMR (101 MHz, $CDCl_3$): δ = 42.1, 42.5, 46.9, 47.5 (4 x NCH_2), 104.4 (m, CH_{Ar}), 112.7 (dd, $J_{C,F}$ = 2 Hz, $J_{C,F}$ = 22 Hz, CH_{Ar}), 119.8 (d, $J_{C,F}$ = 18 Hz, C_{Ar}), 131.0 (m, CH_{Ar}), 158.7 (dt, $J_{C,F}$ = 206 Hz, $J_{C,F}$ = 12 Hz, C_{Ar}), 164.0 (dt, $J_{C,F}$ = 254 Hz, $J_{C,F}$ = 10 Hz, C_{Ar}), 164.7 (d, $J_{C,F}$ = 18 Hz, C = O) ppm; ^{19}F NMR (378 MHz, $CDCl_3$): δ = −110.7 (ArF), −106.0 (ArF) ppm; MS (ESI+): *m*/*z* = 267 $[M+H]^+$.

2.6. Synthesis of N,N-Diethyl-2,4-difluorobenzamide (**4**)

Diethylamine (2 equiv.) was dissolved in absolute chloroform, 2,4-difluorobenzoyl chloride (1 equiv.) was added slowly at 0 °C, and the mixture was allowed to stir at rt overnight. Afterwards, the solvent was removed and the crude mixture of products was purified via automated column chromatography, yielding *N*,*N*-diethyl-2,4-difluorobenzamide (**4**) in 86% yield as a colorless oil. ^{1}H NMR (400 MHz, DMSO-d_6): δ = 1.00 (t, *J* = 7.1 Hz, 3H, CH_3), 1.14 (t, *J* = 7.1 Hz, 3H, CH_3), 3.12 (q, *J* = 7.1 Hz, 2H, NCH_2), 3.45 (q, *J* = 7.1 Hz, 2H, NCH_2), 7.16 (dt, *J* = 2.4 Hz, *J* = 8.6 Hz, 1H, ArH), 7.35 (dt, ^{3}J = 2.5 Hz, $^{3}J_{H,F}$ = 9.8 Hz, 2H, ArH), 7.44 (dd, J = 8.6 Hz, *J* = 14.9 Hz, 1H, ArH) ppm; ^{13}C NMR (101 MHz, DMSO-d_6): δ = 12.8, 13.9 (2 x CH_3), 38.7, 42.6 (2 x NCH_2), 104.4 (t, $J_{C,F}$ = 25.9 Hz, CH_{Ar}), 112.1 (dd, $J_{C,F}$ = 3.5 Hz, $J_{C,F}$ = 21.6 Hz, CH_{Ar}), 121.8 (dd, $J_{C,F}$ = 3.9 Hz, $J_{C,F}$ = 18.9 Hz, C_{Ar}), 129.6 (dd, $J_{C,F}$ = 5.9 Hz, $J_{C,F}$ = 9.9 Hz, CH_{Ar}), 157.8 (dt, $J_{C,F}$ = 246.7 Hz, $J_{C,F}$ = 12.6 Hz, C_{Ar}), 162.3 (dt, $J_{C,F}$ = 248.0 Hz, $J_{C,F}$ = 12.1 Hz, C_{Ar}), 164.1 (C = O) ppm; ^{19}F NMR (378 MHz, DMSO-d_6): δ = −113.1 (ArF), −108.7 (ArF) ppm; MS (ESI+): *m*/*z* = 214 $[M+H]^+$.

2.7. Synthesis of (2,4-Difluorophenyl)(piperidin-1-yl)methanone (**5**)

Piperidine (2 equiv.) was dissolved in absolute chloroform, 2,4-difluorobenzoyl chloride (1 equiv.) was added slowly at 0 °C, and the mixture was allowed to stir at rt overnight. Afterwards, the solvent was removed and the crude mixture of products was purified via automated column chromatography, yielding (2,4-difluorophenyl)(piperidin-1-yl)methanone (**5**) in 82% yield as a colorless oil. ^{1}H NMR (400 MHz, DMSO-d_6): δ = 1.00 (t, *J* = 7.1 Hz, 3H, CH_3), 1.14 (t, *J* = 7.1 Hz, 3H, CH_3), 3.12 (q, *J* = 7.1 Hz, 2H, NCH_2), 3.45 (q, *J* = 7.1 Hz, 2H, NCH_2), 7.16 (dt, *J* = 2.4 Hz, *J* = 8.6 Hz, 1H, ArH), 7.35 (dt, ^{3}J = 2.5 Hz, $^{3}J_{H,F}$ = 9.8 Hz, 2H, ArH), 7.44 (dd, J = 8.6 Hz, *J* = 14.9 Hz, 1H, ArH) ppm; ^{13}C NMR (101 MHz, DMSO-d_6): δ = 12.8, 13.9 (2 x CH_3), 38.7, 42.6 (2 x NCH_2), 104.4 (t, $J_{C,F}$ = 25.9 Hz, CH_{Ar}), 112.1 (dd, $J_{C,F}$ = 3.5 Hz, $J_{C,F}$ = 21.6 Hz, CH_{Ar}), 121.8 (dd, $J_{C,F}$ = 3.9 Hz, $J_{C,F}$ = 18.9 Hz, C_{Ar}), 129.6 (dd, $J_{C,F}$ = 5.9 Hz, $J_{C,F}$ = 9.9 Hz, CH_{Ar}), 157.8 (dt, $J_{C,F}$ = 246.7 Hz, $J_{C,F}$ = 12.6 Hz, C_{Ar}), 162.3 (dt, $J_{C,F}$ = 248.0 Hz, $J_{C,F}$ = 12.1 Hz, C_{Ar}), 164.1 (C = O) ppm; ^{19}F NMR (378 MHz, DMSO-d_6): δ = −113.1 (ArF), −108.7 (ArF) ppm; MS (ESI+): *m*/*z* = 226 $[M+H]^+$.

2.8. Synthesis of (2,4-Difluorophenyl)(morpholino)methanone (**6**)

Morpholine (2 equiv.) was dissolved in absolute chloroform, 2,4-difluorobenzoyl chloride (1 equiv.) was added slowly at 0 °C, and the mixture was allowed to stir at rt overnight. Afterwards, the solvent was removed and the crude mixture of products was purified via automated column chromatography, yielding (2,4-difluorophenyl)(morpholino)methanone (**6**) in 87% yield as a colorless oil. ^{1}H NMR (400 MHz, DMSO-d_6): δ = 3.23 (t, *J* = 4.5 Hz, 2H, NCH_2), 3.52 (t, *J* = 4.5 Hz, 2H, NCH_2), 3.64 (s, 4H, OCH_2), 7.19 (dt, *J* = 2.3 Hz, *J* = 8.5 Hz, 1H, ArH), 7.36 (dt, ^{3}J = 2.3 Hz, $^{3}J_{H,F}$ = 9.9 Hz, 2H, ArH), 7.50 (dd, *J* = 8.3 Hz, *J* = 14.8 Hz, 1H, ArH) ppm; ^{13}C NMR (101 MHz, DMSO-d_6): δ = 41.9, 47.0 (2 x NCH_2), 65.9, 66.2 (2 x OCH_2), 104.4 (t, $J_{C,F}$ = 26.0 Hz, CH_{Ar}), 112.3 (dd, $J_{C,F}$ = 3.5 Hz, $J_{C,F}$ = 21.6 Hz, CH_{Ar}), 120.4 (dd, $J_{C,F}$ = 3.9 Hz, $J_{C,F}$ = 18.1 Hz, C_{Ar}), 130.5 (dd, $J_{C,F}$ = 5.6 Hz, $J_{C,F}$ = 10.1 Hz, CH_{Ar}), 158.0 (dt, $J_{C,F}$ = 248.2 Hz, $J_{C,F}$ = 12.8 Hz, C_{Ar}), 162.8 (dt, $J_{C,F}$ = 248.9 Hz, $J_{C,F}$ = 12.1 Hz, C_{Ar}), 163.3 (C = O) ppm; ^{19}F NMR (378 MHz, DMSO-d_6): δ = −112.0 (ArF), −107.8 (ArF) ppm; MS (ESI+): *m*/*z* = 267 $[M+K+H]^+$.

3. Results and Discussion

3.1. Synthesis of the Piperazine Compounds

A one-pot reaction procedure using low-cost starting materials was applied. An excess of piperazine (**2**) was reacted with 2,4-difluorobenzoyl chloride (**1**) in anhydrous chloroform at 0 °C to obtain both compounds, the *N*-monoacylated amide **3a** and the *N*,*N*-diacylated

diamide **3b**, according to a previously published procedure [47]. Depending on the excess of piperazine used for the reaction, compound **3a** was obtained in 66% yield (five-fold excess) and compound **3b** in 44% yield (two-fold excess). The reaction for both piperazines, **3a** and **3b**, is illustrated in Scheme 1.

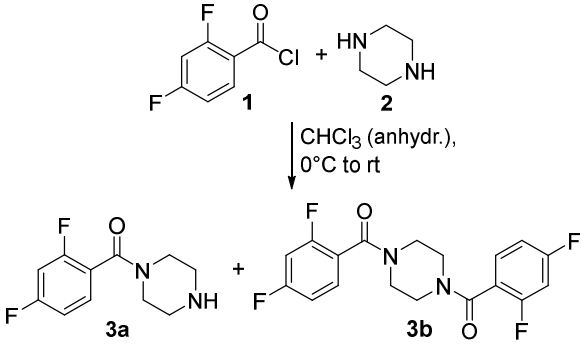

Scheme 1. Preparation of the 2,4-difluoro derivatives **3a** and **3b**.

3.2. Dynamic VT-NMR Study for the Dimer **3b**

During the full characterization of compound **3b**, four broad singlets were observed in the aliphatic region of the ^{1}H NMR spectrum when measured at 25 °C (e.g., for $CDCl_3$: δ = 3.34, 3.44, 3.79, and 3.89 ppm, ratio: 1:1.4:1.4:1 in Figure S10). Normally, one summarized signal could be expected for the NCH_2-protons under these conditions due to the symmetry of the molecule. The ^{1}H NMR spectrum is even more complex when measured at −10 °C. The four signals are again split in a more complicated pattern (see SI) due to the unsymmetrical substitution pattern of the benzene ring. Generally, rotation isomers are possible as shown in Figure 2, when additionally considering the rotation around the C(O)-C_{Ar}-bond.

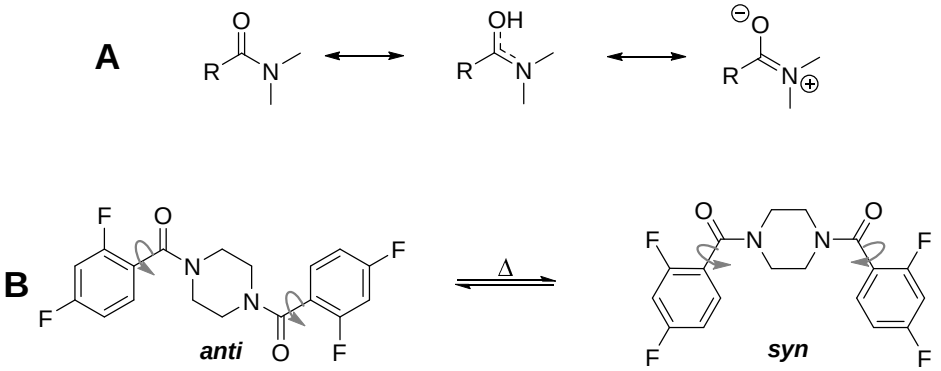

Figure 2. (**A**) partial double bond of amides (**B**) *syn* and *anti* isomer of compound **3b** with free rotation about the single bond (gray arrows).

Supplementary ^{1}H NMR spectra were recorded in DMSO-d_6, methanol-d_4, acetonitrile-d_3, acetone-d_6, benzene-d_6, and tetrachloroethane-d_2 (TCE-d_2) (Figure 3), all showing four signals for the piperazine protons at 25 °C independent of the solvent but with different $\Delta\nu$ values and different integral values. H,H-COSY spectra measured in $CDCl_3$ revealed that only the inner two NCH_2 signals couple (Figure S12). The inner two signals belong to the *anti* (*trans*) isomer (3.43 and 3.79 ppm), whereas the two outer NCH_2 signals belong to the *syn* (*cis*) isomer (3.34 and 3.89 ppm), as indicated by recent results [10,47]. This splitting can also be observed in the ^{13}C NMR spectrum (see Figure S11) with δ = 42.1 and 47.5 ppm for the *syn* isomer and 42.5 and 46.9 ppm for the *anti*-isomer measured in $CDCl_3$. However, a

reduced rotation around the C(O)-C_{Ar}-bond has not been detected at temperatures > 25 °C, only the reduced rotation around the amide bond.

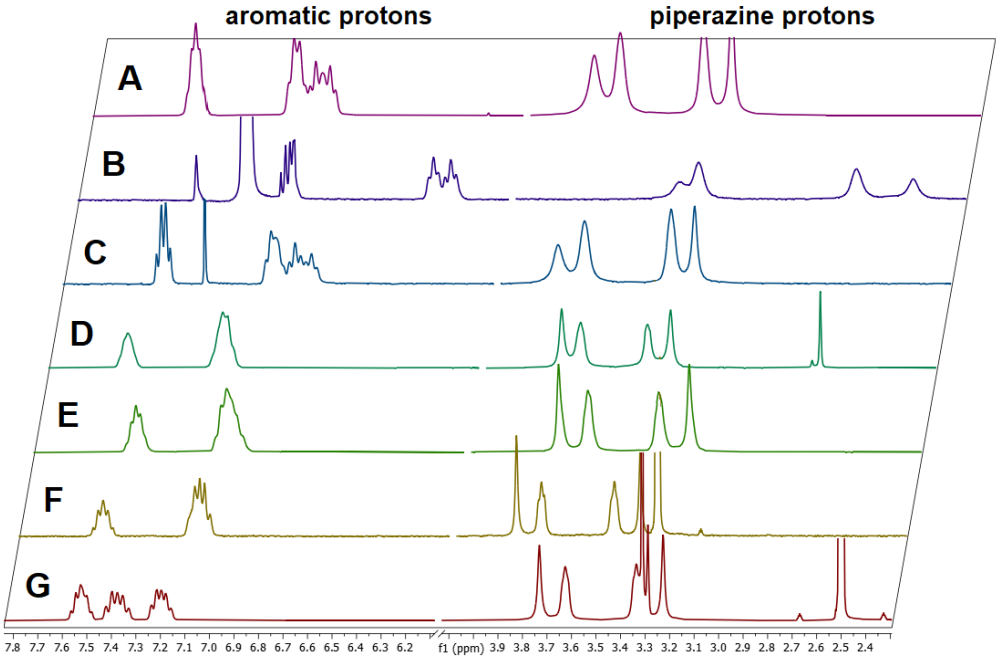

Figure 3. ^{1}H NMR spectra (aliphatic region with piperazine protons from 2.3–4.0 ppm and aromatic region from 6.1–7.8 ppm) of compound **3b** measured in five different solvents: (A) TCE-d_2, (B) benzene-d_6, (C) $CDCl_3$, (D) acetone-d_6, (E) acetonitrile-d_3, (F) methanol-d_4 and (G) DMSO-d_6.

VT-dependent NMR measurements were accomplished (see SI Figures S15–S18) to determine the coalescence point expressed as T_C for the partial amide double bond, which is dependent on the solvent. By warming the NMR sample of **3b**, all four signals with an integration value of two hydrogen atoms each combine to one signal with a value of 8 at the T_C due to the unhindered rotation of the amide bonds beyond this temperature. When using the standard NMR solvent $CDCl_3$, the coalescence point could not be reached due to the boiling point of the solvent (Figure S15). To overcome this, the solvent was changed to tetrachloroethane-d_2 (TCE-d_2) with similar properties but with a boiling point of 145 °C. The VT-dependent ^{1}H NMR spectra are pointed out in Figure 4A, and the T_C was determined at 83 °C. Additionally, VT-^{1}H-NMR spectra were recorded in acetonitrile-d_3 with a T_C of 80 °C and in DMSO-d_6 with a T_C of 83 °C (Figure 4B,C).

The T_C for compound **3b** containing the fluorine 2,4-substitution is higher in all used solvents as for the mono-fluorinated 4-fluorobenzamide compound (T_C = 296 K in $CDCl_3$) and the unsubstituted benzamide compound (T_C = 306 K in $CDCl_3$) due to the higher electron-withdrawing effect caused by the additional fluorine in the *ortho* position of the benzoyl moiety, which strengthens the partial double bond. The higher T_C also has an influence on $\Delta G^{\#}$, which was determined with >68 kJ/mol (*anti*-isomer) and >70 kJ/mol (*syn* isomer) for compound **3b** (see Table 1).

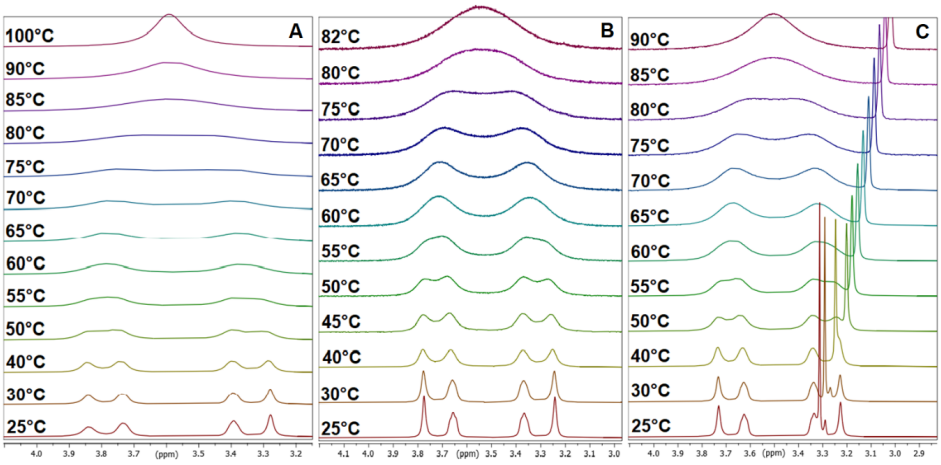

Figure 4. VT-^{1}H NMR spectra of **3b** showing the piperazine protons measured in (**A**) TCE-d_2, (**B**) acetonitrile-d_3, and (**C**) DMSO-d_6 (only the region of the piperazine protons is shown; full spectra see Figures S16–S18).

Table 1. Physicochemical data for compound **3b** in dependence on the solvent. a: anti/s: syn.

Solvent	Ratio *syn*/*anti*	Δν [Hz]	k_{exc} [Hz]	T_C [K]	ΔG‡ [kJ/mol]
Benzene-d_6	1.5:1	257 (a) 381 (s)	313 (a) 494 (s)	n.d.	- -
$CDCl_3$	1.2:1	141 (a) 223 (s)	244 (a) 395 (s)	n.d.	- -
TCE-d_2	1.1:1	136 (a) 224 (s)	571 (a) 846 (s)	356	70.8 69.3
Acetone-d_6	1.2:1	110 (a) 223 (s)	302 (a) 498 (s)	n.d.	- -
ACN-d_3	1.1:1	116 (a) 213 (s)	258 (a) 473 (s)	353	70.7 68.9
CD_3OD	1.1:1	119 (a) 202 (s)	264 (a) 448 (s)	n.d.	- -
DMSO-d_6	1.2:1	116 (a) 202 (s)	258 (a) 448 (s)	353	70.7 69.0

A 2D ^{1}H EXSY spectrum was recorded at 25 °C and 600 ms mixing time, showing the exchange of the protons (representative for compound **3b** in Figure 5). At this temperature, the molecule exhibits slow rotation around the N-C bond such that both groups exchange with one another rotationally yet are distinct in the spectrum.

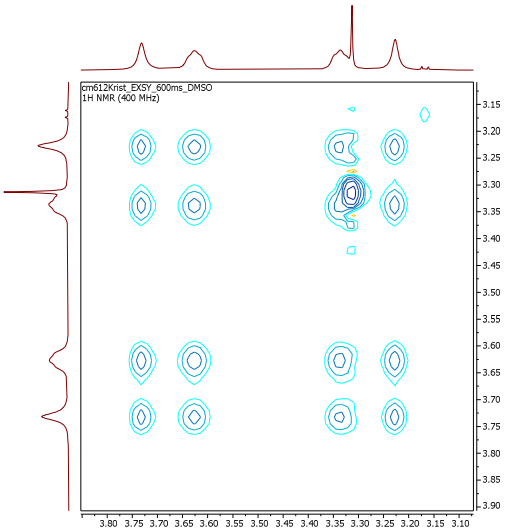

Figure 5. Representative 2D ^{1}H EXSY spectrum of **3b** in DMSO-d_6 at 25 °C with 600 ms mixing time.

3.3. X-Ray Structure Analysis of **3b**

Single crystals of **3b** were obtained, and the crystal and molecular structure were determined using single-crystal X-ray structure analysis. The molecular structure of this compound and the atom numbering scheme are shown in Figure 6. Relevant crystallographic data is given in Table 2.

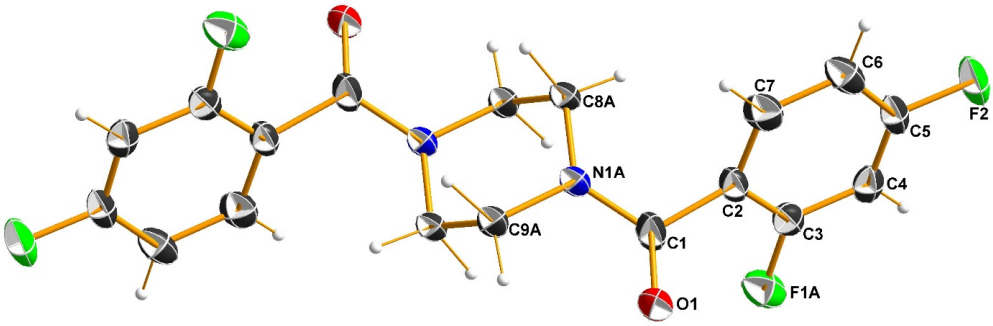

Figure 6. Molecular structure of the compound **3b** (ORTEP plot with 50% probability level, the respective second orientations of the disordered piperazine moiety and the F1/F1A atom are not shown for better visibility; see Figure 7).

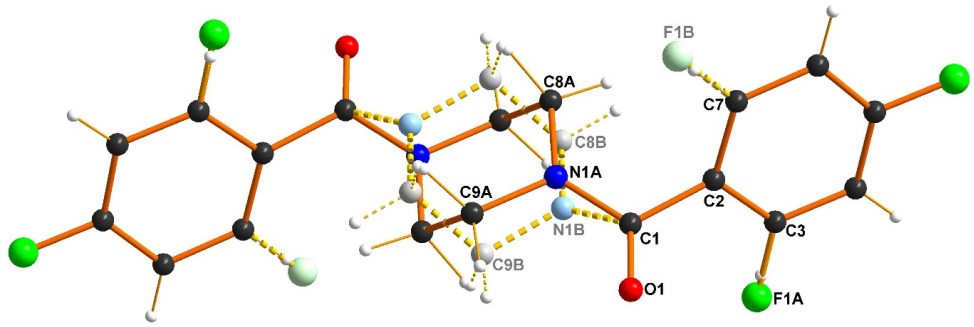

Figure 7. Superimposition of the different disordered moieties in crystals of **3b**, discriminated by the labels A and B, different color intensities, and solid/dashed lines.

Table 2. Crystal data and structure refinement for compound **3b**.

Compound	3b
Formula	$C_{18}H_{14}F_4N_2O_2$
Formula weight (g·mol^{-1})	366.31
Temperature (K)	123
Crystal system	monoclinic
Space group	$P2_1/c$
Unit cell dimensions:	
a (Å)	7.2687(3)
b (Å)	17.2658(8)
c (Å)	6.9738(3)
β (°)	115.393(2)
Volume (Å^3), Z	790.65(6), 2
Data/restraints/param.	2955/0/157
Measured reflections	23,516
$2\theta_{max}$ (°)	66.0
GoF on F^2	1.08
R1 [$I > 2\sigma(I)$]	0.058
$wR2$ (all data)	0.154
Larg. diff. peak/hole (e·Å^3)	0.36/−0.31

Compound **3b** crystallizes in the monoclinic crystal system with the space group $P2_1/c$. The asymmetric unit consists of one half of a molecule. It is located such that the center of the piperazine ring is positioned on the inversion center, i.e., the molecule has an inversion symmetry. In the crystal, parts of the molecules of **3b** are arranged with different orientations, i.e., they are disordered. The *ortho*-located fluorine atom (F1) is either *cis* (F1A) or *trans* (F2B) oriented with respect to the oxygen atom O1 (see *anti*-isomers in Figure 2). The occupation of the F1A site has been refined to 26.5%. The piperazine moiety has two different orientations, A and B, as shown in Figure 6, with an occupancy of 56.4% for orientation A. As visible in Figures 6 and 7, only the *anti*-conformer (with respect to the orientation of the two oxygen atoms in each molecule) exists in the solid state. This probably results from intermolecular interactions preferring this orientation in the solid state, which are not present in solution.

The bonding environment around the nitrogen atom N1A (and also around N1B, respectively) is close to a trigonal planar disposition. The average bond angle of 119.7° and the distance of N1A to the plane of the three surrounding C atoms of only 0.08 Å indicate that the C1−N1A bond has at least a strong partial double bond character. Additionally, this bond is significantly shorter (1.398(2) Å) than comparable aliphatic bonds (i.e., 1.462(4) Å in *N*-methylpiperazine(sulfan)). These structural features are consistent with the NMR data, as shown above. The CH_2 groups of the piperazine moiety have bond angles close to tetrahedral, as expected, with H−C−C−H dihedral angles of 53.3° and −65.2°.

3.4. Dynamic NMR Studies of Monomer **3a**

The mono-substituted 2,4-fluorobenzyl compound **3a**, with only one amide site and one free secondary amine site, shows a similar splitting behavior. Four signals for NCH_2 groups are observed in the ^{1}H NMR spectrum at 25 °C measured in $CDCl_3$ (Figure S1); two for the amide site (δ = 3.39 and 3.85 ppm) and two for the amine site (δ = 2.92 and 3.03 ppm). The evaluation of a H,H-COSY spectrum (Figure S3) showed again the independent coupling of two NCH_2 groups.

Two effects can be discussed for the splitting of the piperazine signals. The first effect is related to the limited rotation around the amide bond (as discussed above), and the second effect is related to the interconversion of two piperazine ring chair conformations [47], which occurs at deeper temperatures and thus did not have an influence. When measuring VT-dependent ^{1}H NMR spectra in $CDCl_3$ (Figure S7), only the T_C of the amine site was detectable at 57 °C; the coalescence temperature of the amide site is located above the boiling point of the solvent. Thus, TCE-d_2 and DMSO-d_6 were again used as solvents (Figure 8), having T_Cs for the amine site of 63 °C and 61 °C, respectively, and for the amide site of 82 °C and 79 °C, respectively. All T_C values are higher compared to the respective monosubstituted 4-fluorobenzoyl compound ($T_{C,amine}$ = 25 °C, $T_{C,amide}$ = 36 °C) due to the additional fluorine atom in the 2-position of the ring, which triggers a higher double bond character of the amide bond. As a result, the Gibbs free activation energy $\Delta G^‡$ is also higher for the 2,4-difluoro compound **3a** in comparison to the respective 4-fluorobenzoyl compound ($\Delta G^‡$ = 60.4 kJ/mol), but the solvent seems to have only a small influence on the rotation. All results concerning compound **3a** are summarized in Table 3.

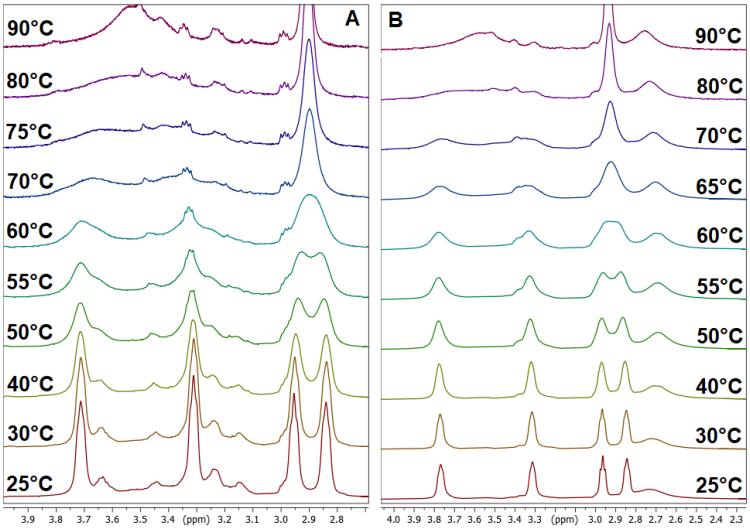

Figure 8. VT-^{1}H NMR spectra of **3a** measured in (**A**) DMSO-d_6 and (**B**) TCE-d_2 (region of the piperazine protons is shown; see Figures S8 and S9 for full spectra).

Table 3. Physicochemical parameters of compound **3a**.

Solvent	Δν [Hz]	k_{exc} [Hz]	T_C [K]	ΔG‡ [kJ/mol]
$CDCl_3$	45	100 (amine)	330 (amine)	68.5
	185	411 (amide)	n.d. (amide)	-
TCE-d_2	48	107 (amine)	336 (amine)	69.6
	160	355 (amide)	355 (amide)	70.1
DMSO-d_6	46	102 (amine)	334 (amine)	69.3
	160	355 (amide)	352 (amide)	69.5

3.5. Comparison with Other 2,4-Difluorobenzamides

To compare the results of compounds **3a** and **3b** and to study the influence of the organic groups connected at the amide nitrogen atom (open chain or cyclic or, with or without heteroatom), three additional 2,4-difluorobenzamides **4**–**6** were prepared (Figure 9) with diethyl (**4**), piperidinyl (**5**) and morpholinyl (**6**) as substituents according to the synthesis of **3a** and **3b** with 2,4-difluorobenzyl chloride (**1**) and the respective amines in anhydrous chloroform.

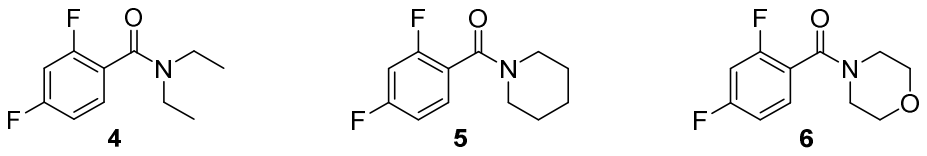

Figure 9. Selected 2,4-difluorobenzamides **4**–**6** with different amide functions (diethyl, piperidinyl, morpholinyl).

All NMR spectra were recorded in DMSO-d_6 (Figure 10), and all compounds **4**–**6** nicely show the splitting of the amide residues due to the hindered rotation around the C(O)-N bond (Figure 10). Again, VT-^{1}H-NMR spectra were recorded for compounds **4**–**6** in DMSO-d_6 (Figures S27, S36, and S45) to determine the Tc's of the compounds for the calculation of the rotation barrier according to equations (1) and (2). All recorded data and calculated energy barriers expressed as Gibbs energy ΔG‡ were found in Table 4. The chosen organic groups of the amide site do not have a big influence on the rotation. The highest barrier with 73.9 kJ/mol was found for the open-chain diethylamide **4**. Overall, all calculated energy

values for the rotation barrier of **3a**, **3b**, and **4**–**6** are in the same range. The additional fluorine in the 2-position of the aromatic ring primarily influences the rotation barrier.

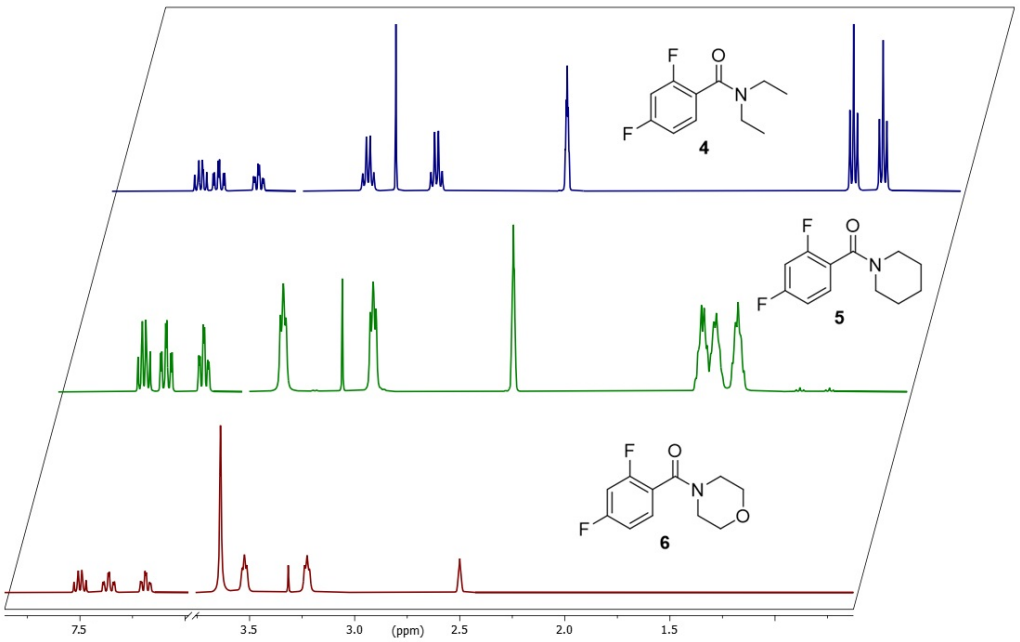

Figure 10. Comparison of ^{1}H NMR spectra (aliphatic region and aromatic region) of compounds **4** (diethyl), **5** (piperidinyl) and **6** (morpholinyl) measured in DMSO-d_6 at 25 °C.

Table 4. Physicochemical parameters of compounds **3a**, **3b,** and **4**–**6** measured in DMSO-d_6.

Compound	Δν [Hz]	k_{exc} [Hz]	T_C [K]	ΔG‡ [kJ/mol]
3a	116 (*anti*) 202 (*syn*)	258 (*anti*) 448 (*syn*)	353	70.7 69.0
3b	48 (amine) 160 (amide)	107 (amine) 355 (amide)	336 (amine) 355 (amide)	69.6 70.1
4	56 (CH_3) 130 (CH_2)	124 (CH_3) 289 (CH_2)	358 (CH_3) 370 (CH_2)	73.9 73.8
5	171 (amide) 41 (CH_2)	380 (amide) 91 (CH_2)	371 348	73.2 72.6
6	119	264	361	72.2

4. Conclusions

Two fluorine-containing piperazine derivatives **3a** and **3b** were synthesized using a convenient one-pot synthesis procedure. An evaluation of the NMR spectra showed four signals of the NCH_2 groups of the piperazine moiety for both compounds, coming from the formation of different rotation isomers. An existing partial double bond in the amide residue led to rotational conformers, whereas the ring conversion of the amine site in **3a** and additional reduced rotation around the C(O)-C_{Ar}-bond in **3a** and **3b** are not observed at temperatures > 25 °C. To investigate the influence of the organic groups of the amide, three additional compounds **4**–**6** were prepared, and VT-^{1}H-NMR spectra were recorded in DMSO-d_6. Activation energies $\Delta G^{\ddagger}_{exc}$ were calculated from solvent-dependent coalescence temperatures T_C, which are all in the same range between 69 and 73 kJ/mol. They are higher compared to the mono-fluorinated amide and to the unsubstituted benzamide. The formation of conformers of compound **3b**, which result from the partial double bond, was additionally determined and verified using single-crystal X-ray structure analysis for this compound. Only a minor influence of the solvent was observed.

Supplementary Materials: The following supporting information can be downloaded at: https://www.mdpi.com/article/10.3390/chemistry7050162/s1. Figure S1: ^{1}H NMR spectrum of compound **3a** in $CDCl_3$; Figure S2: ^{13}C NMR spectrum of compound **3a** in $CDCl_3$; Figure S3: H,H-COSY spectrum of compound **3a** in $CDCl_3$; Figure S4: H,C-HSQC spectrum of compound **3a** in $CDCl_3$; Figure S5: IR spectrum of compound **3a**; Figure S6: Mass spectrum (ESI+) of compound **3a**; Figure S7: ^{1}H-VT-NMR spectra of **3a** measured in $CDCl_3$; Figure S8: ^{1}H-VT-NMR spectra of **3a** measured in TCE-d_2; Figure S9: ^{1}H-VT-NMR spectra of **3a** measured in DMSO-d_6; Figure S10: ^{1}H NMR spectrum of compound **3b** in $CDCl_3$; Figure S11: ^{13}C NMR spectrum of compound **3b** in $CDCl_3$; Figure S12: H,H-COSY spectrum of compound **3b** in $CDCl_3$; Figure S13: H,C-HSQC spectrum of compound **3b** in $CDCl_3$; Figure S14: EXSY spectrum of compound **3b** (mixing time 600 ms, T = 25 °C) in DMSO-d_6; Figure S15: ^{1}H-VT-NMR spectra of **3b** in $CDCl_3$; Figure S16: ^{1}H-VT-NMR spectra of **3b** in TCE-d_2; Figure S17: ^{1}H-VT-NMR spectra of **3b** in ACN-d_3; Figure S18: ^{1}H-VT-NMR spectra of **3b** in DMSO-d_6; Figure S19: ^{1}H NMR spectrum of compound **4** in DMSO-d_6; Figure S20: ^{13}C NMR spectrum of compound **4** in DMSO-d_6; Figure S21: H,H-COSY spectrum of compound **4** in DMSO-d_6; Figure S22: H,C-HSQC spectrum of compound **4** in DMSO-d_6; Figure S23: ^{19}F NMR spectrum of compound **4** in DMSO-d_6; Figure S24: EXSY spectrum of compound **4** (mixing time 600 ms, T = 25 °C) in DMSO-d_6; Figure S25: IR spectrum of compound **4**; Figure S26: Mass spectrum (ESI+) spectrum of compound **4**; Figure S27: ^{1}H-VT-NMR spectra of **4** in DMSO-d_6; Figure S28: ^{1}H NMR spectrum of compound **5** in DMSO-d_6; Figure S29: ^{13}C NMR spectrum of compound **5** in DMSO-d_6; Figure S30: H,H-COSY spectrum of compound **5** in DMSO-d_6; Figure S31: H,C-HSQC spectrum of compound **5** in DMSO-d_6; Figure S32: EXSY spectrum of compound **5** (mixing time 600 ms, T = 25 °C) in DMSO-d_6; Figure S33: ^{19}F NMR spectrum of compound **5** in DMSO-d_6; Figure S34: IR spectrum of compound **5**; Figure S35: Mass spectrum (ESI+) of compound **5**; Figure S36: ^{1}H-VT-NMR spectra of **5** in DMSO-d_6; Figure S37: ^{1}H NMR spectrum of compound **6** in DMSO-d_6; Figure S38: ^{13}C NMR spectrum of compound **6** in DMSO-d_6; Figure S39: H,H-COSY spectrum of compound **6** in DMSO-d_6; Figure S40: H,C-HSQC spectrum of compound **6** in DMSO-d_6; Figure S41: EXSY spectrum of compound **6** (mixing time 600 ms, T = 25 °C) in DMSO-d_6; Figure S42: Figure S43: IR spectrum of compound **6**; Figure S44: Mass spectrum (ESI+) of compound **6**; ^{19}F NMR spectrum of compound **6** in DMSO-d_6; Figure S45: ^{1}H-VT-NMR spectra of **6** in DMSO-d_6.

Author Contributions: Conceptualization, C.M.; methodology, M.K. and C.M.; validation, M.K. and C.M.; formal analysis, M.K. and C.M.; investigation, C.M.; resources, M.K. and C.M.; data curation, M.K. and C.M.; writing—original draft preparation, M.K. and C.M.; writing—review and editing, M.K. and C.M.; visualization, M.K. and C.M. All authors have read and agreed to the published version of the manuscript.

Funding: This research received no external funding.

Data Availability Statement: The raw data is archived at the HZDR database and will be made available upon request.

Conflicts of Interest: The authors declare no conflicts of interest.

Abbreviations

The following abbreviations are used in this manuscript:

ACN	Acetonitrile
COSY	Correlation spectroscopy
DMSO	Dimethyl sulfoxide
EXSY	Exchange spectroscopy
TCE	1,1,2,2-Tetrachloroethane
TLC	Thin-layer chromatography
VT	Variable temperature
XRD	X-ray diffraction

References

1. Gettys, K.E.; Ye, Z.; Dai, M. Recent Advances in Piperazine Synthesis. *Synthesis* **2017**, *49*, 2589–2604. [CrossRef]
2. Zhang, R.H.; Guo, H.Y.; Deng, H.; Li, J.; Quan, Z.S. Piperazine skeleton in the structural modification of natural products: A review. *J. Enzyme Inhib. Med. Chem.* **2021**, *36*, 1165–1197. [CrossRef] [PubMed]
3. Marshall, C.M.; Federice, J.G.; Bell, C.N.; Cox, P.B.; Njardarson, J.T. An Update on the Nitrogen Heterocycle Compositions and Properties of U.S. FDA-Approved Pharmaceuticals (2013–2023). *J. Med. Chem.* **2024**, *67*, 11622–11655. [CrossRef] [PubMed]
4. Faizan, M.; Kumar, R.; Mazumder, A.; Salahuddin; Kukreti, N.; Kumar, A.; Chaitanya, M.V.N.L. The medicinal chemistry of piperazines: A review. *Chem. Biol. Drug Des.* **2024**, *103*, e14537. [CrossRef] [PubMed]
5. Heravi, M.M.; Zadsirjan, V. Prescribed drugs containing nitrogen heterocycles: An overview. *RSC Adv.* **2020**, *10*, 44247–44311. [CrossRef]
6. Dömling, A.; Huang, Y. Piperazine Scaffolds via Isocyanide-Based Multicomponent Reactions. *Synthesis* **2010**, *17*, 2859–2883. [CrossRef]
7. Durand, C.; Szostak, M. Recent Advances in the Synthesis of Piperazines: Focus on C–H Functionalization. *Organics* **2021**, *2*, 337–347. [CrossRef]
8. Huang, Z.; Shi, W. UV curing behavior of hyperbranched polyphosphate acrylate/di(hydroxylpropyl methacrylate) piperazine and properties of the cured film. *Prog. Org. Coat.* **2007**, *59*, 312–317. [CrossRef]
9. Zhao, B.; Xiao, Y.; Yuan, D.; Lu, C.; Yao, Y. Synthesis and characterization of bridged bis(amidato) rare earth metal amides and their applications in C–N bond formation reactions. *Dalton Trans.* **2016**, *45*, 3880–3887. [CrossRef]
10. Sahoo, H.S.; Chand, D.K. Conformation of *N,N′*-bis(3-pyridylformyl)piperazine and spontaneous formation of a saturated quadruple stranded metallohelicate. *Dalton Trans.* **2010**, *39*, 7223–7225. [CrossRef]
11. Barnes, D.J.; Chapman, R.L.; Vagg, R.S.; Watton, E.C. Synthesis of novel bis(amides) by means of triphenyl phosphite intermediates. *J. Chem. Eng. Data* **1978**, *23*, 349–350. [CrossRef]
12. Andronati, S.A.; Karaseva, T.L.; Krysko, A.A. Peptidomimetics-antagonists of the fibrinogen receptors: Molecular design, structures, properties and therapeutic applications. *Curr. Med. Chem.* **2004**, *11*, 1183–1211. [CrossRef] [PubMed]
13. Horton, D.A.; Bourne, G.T.; Smythe, M.L. Exploring privileged structures: The combinatorial synthesis of cyclic peptides. *Mol. Divers.* **2000**, *5*, 289–304. [CrossRef]
14. Wodtke, R.; König, J.; Pigorsch, A.; Köckerling, M.; Mamat, C. Evaluation of novel fluorescence probes for conjugation purposes using the traceless Staudinger Ligation. *Dyes Pigment.* **2015**, *113*, 263–273. [CrossRef]
15. Heldt, J.-M.; Kerzendörfer, O.; Mamat, C.; Starke, F.; Pietzsch, H.-J.; Steinbach, J. Synthesis of Short and Versatile Heterobifunctional Linkers for Conjugation Purposes of Bioactive Molecules with (Radio-)Labels. *Synlett* **2013**, *24*, 432–436. [CrossRef]
16. Lemoucheux, L.; Rouden, J.; Ibazizene, M.; Sobrio, F.; Lasne, M.C. Debenzylation of Tertiary Amines Using Phosgene or Triphosgene: An Efficient and Rapid Procedure for the Preparation of Carbamoyl Chlorides and Unsymmetrical Ureas. Application in Carbon-11 Chemistry. *J. Org. Chem.* **2003**, *68*, 7289–7297. [CrossRef]
17. Grosse-Gehling, P.; Wuest, F.R.; Peppel, T.; Köckerling, M.; Mamat, C. [^{18}F]1-(3-fluoropropyl)piperazines as model compounds for the radiofluorination of pyrido [2,3-*d*]pyrimidines. *Radiochim. Acta* **2011**, *99*, 365. [CrossRef]
18. Pretze, M.; Mamat, C. Automated preparation of [^{18}F]AFP and [^{18}F]BFP: Two novel bifunctional 18F-labeling building blocks for Huisgen-click. *J. Fluor. Chem.* **2013**, *150*, 25–35. [CrossRef]
19. Mamat, C.; Pretze, M.; Gott, M.; Köckerling, M. Synthesis, dynamic NMR characterization and XRD studies of novel *N,N′*-substituted piperazines for bioorthogonal labeling. *Beilstein J. Org. Chem.* **2016**, *12*, 2478–2489. [CrossRef]
20. Wiemer, J.; Steinbach, J.; Pietzsch, J.; Mamat, C. Preparation of a novel radiotracer targeting the EphB4 receptor via radiofluorination using spiro azetidinium salts as precursor. *J. Labelled Comp. Radiopharm.* **2017**, *60*, 489–498. [CrossRef]
21. Katz, D.P.; Deruiter, J.; Bhattacharya, D.; Ahuja, M.; Bhattacharya, S.; Clark, C.R.; Suppiramaniam, V.; Dhanasekaran, M. Benzylpiperazine: "A messy drug". *Drug Alcohol Depend.* **2016**, *164*, 1–7. [CrossRef]
22. Shaquiquzzaman, M.; Verma, G.; Marella, A.; Akhter, M.; Akhtar, W.; Khan, M.F.; Tasneem, S.; Alam, M.M. Piperazine scaffold: A remarkable tool in generation of diverse pharmacological agents. *Eur. J. Med. Chem.* **2015**, *102*, 487–529. [CrossRef] [PubMed]
23. Shen, L.; Ye, Y.H.; Wang, X.T.; Zhu, H.L.; Xu, C.; Song, Y.C.; Li, H.; Tan, R.X. Structure and total synthesis of aspernigerin: A novel cytotoxic endophyte metabolite. *Chem. Eur. J.* **2006**, *12*, 4393–4396. [CrossRef] [PubMed]
24. Irikura, T.; Masuzawa, K.; Nishino, K.; Kitagawa, M.; Uchida, H.; Ichinoseki, N.; Ito, M. New analgetic agents. V. 1-butyryl-4-cinnamylpiperazine hydrochloride and related compounds. *J. Med. Chem.* **1968**, *11*, 801–804. [CrossRef] [PubMed]
25. Rathi, A.K.; Syed, R.; Shin, H.S.; Patel, R.V. Piperazine derivatives for therapeutic use: A patent review (2010–present). *Expert Opin. Ther. Pat.* **2016**, *26*, 777–797. [CrossRef]
26. Abou El-Ella, D.A.; Hussein, M.M.; Serya, R.A.; Abdel Naby, R.M.; Al-Abd, A.M.; Saleh, D.O.; El-Eraky, W.I.; Abouzid, K.A. Molecular design and synthesis of 1,4-disubstituted piperazines as α(1)-adrenergic receptor blockers. *Bioorg. Chem.* **2014**, *54*, 21–30. [CrossRef]

27. Patel, R.V.; Park, S.W. An evolving role of piperazine moieties in drug design and discovery. *Mini-Rev. Med. Chem.* **2013**, *13*, 1579–1601. [CrossRef]
28. Miniyar, P.B.; Murumkar, P.R.; Patil, P.S.; Barmade, M.A.; Bothara, K.G. Unequivocal role of pyrazine ring in medicinally important compounds: A review. *Mini-Rev. Med. Chem.* **2013**, *13*, 1607–1625. [CrossRef]
29. Font, M.; Ardaiz, E.; Cordeu, L.; Cubedo, E.; Garcia-Foncillas, J.; Sanmartin, C.; Palop, J.A. Structural characteristics of novel symmetrical diaryl derivatives with nitrogenated functions. Requirements for cytotoxic activity. *Bioorg. Med. Chem.* **2006**, *14*, 1942–1948. [CrossRef]
30. Radin, D.P.; Lippa, A.; Rana, S.; Fuller, D.D.; Smith, J.L.; Cerne, R.; Witkin, J.M. Amplification of the therapeutic potential of AMPA receptor potentiators from the nootropic era to today. *Pharmacol. Biochem. Behav.* **2025**, *248*, 173967. [CrossRef]
31. Rana, S.; Fusco, A.F.; Witkin, J.M.; Radin, D.P.; Cerne, R.; Lippa, A.; Fuller, D.D. Pharmacological modulation of respiratory con-trol: Ampakines as a therapeutic strategy. *Pharmacol. Ther.* **2025**, *265*, 108744. [CrossRef]
32. Czopek, A.; Kubacka, M.; Bucki, A.; Siwek, A.; Filipek, B.; Pawłowski, M.; Kołaczkowski, M. Novel serotonin 5-HT_{2A} receptor antagonists derived from 4-phenylcyclohexane-5-spiro-and 5-methyl-5-phenyl-hydantoin, for use as potential antiplatelet agents. *Pharmacol. Rep.* **2021**, *73*, 1361–1372. [CrossRef]
33. Liu, X.-K.; Ma, L.-X.; Wei, Z.-Y.; Cui, X.; Zhan, S.; Yin, X.-M.; Piao, H.-R. Synthesis and Positive Inotropic Activity of [1,2,4]Triazolo [4,3-a] Quinoxaline Derivatives Bearing Substituted Benzylpiperazine and Benzoylpiperazine Moieties. *Molecules* **2017**, *22*, 273. [CrossRef]
34. Moorman, A.R. Adenosine a2a Receptor Antagonists. U.S. Patent 2008242672A1, 6 April 2010.
35. Dong, H.; Zhang, L. Pyridino-Pyrimidine Compound and Application Thereof. CN Patent 109748914A, 25 May 2025.
36. Arkinstall, S.; Halazy, S.; Church, D.; Camps, M.; Rueckle, T.; Gotteland, J.P.; Biamonte, M. Pharmaceutically Active Sulfonamide Derivatives. U.S. Patent 8012995B1, 6 September 2011.
37. Ielo, L.; Deri, B.; Germanò, M.P.; Vittorio, S.; Mirabile, S.; Gitto, R.; Rapisarda, A.; Ronsisvalle, S.; Floris, S.; Pazy, Y.; et al. Exploiting the 1-(4-fluorobenzyl)piperazine fragment for the development of novel tyrosinase inhibitors as anti-melanogenic agents: Design, synthesis, structural insights and biological profile. *Eur. J. Med. Chem.* **2019**, *178*, 380–389. [CrossRef] [PubMed]
38. Wang, J.Q.; Yang, M.D.; Chen, X.; Wang, Y.; Chen, L.Z.; Cheng, X.; Liu, X.H. Discovery of new chromen-4-one derivatives as telomerase inhibitors through regulating expression of dyskerin. *J. Enzyme. Inhib. Med. Chem.* **2018**, *33*, 1199–1211. [CrossRef] [PubMed]
39. Ghosh, K.K.; Jeong, Y.M.; Kang, N.Y.; Lee, J.; Diana, W.S.Y.; Kim, J.Y.; Yoo, J.; Kim, D.; Kim, Y.K.; Chang, Y.T. The development of a nucleus staining fluorescent probe for dynamic mitosis imaging in live cells. *Chem. Commun.* **2015**, *51*, 9336–9338. [CrossRef] [PubMed]
40. Ha, H.H.; Kim, J.S.; Kim, B.M. Novel heterocycle-substituted pyrimidines as inhibitors of NF-κB transcription regulation related to TNF-α cytokine release. *Bioorg. Med. Chem. Lett.* **2008**, *18*, 653–656. [CrossRef]
41. Dugave, C.; Demange, L. Cis−Trans Isomerization of Organic Molecules and Biomolecules: Implications and Applications. *Chem. Rev.* **2003**, *103*, 2475–2532. [CrossRef]
42. Jackman, L.M.; Kavanagh, T.E.; Haddon, R.C. Studies in nuclear magnetic resonance—IX. Rotational barriers in substituted *N*,*N*-dimethylbenzamides. *Org. Magn. Reson.* **1969**, *1*, 109–123. [CrossRef]
43. Alberghina, G.; Bottino, F.A.; Fisichella, S.; Arnone, C. Solvent effects on the rotational barriers of the *N*,*N*-dimethylamides of 2- and 3-furoic and 2- and 3-thenoic acids. *J. Chem. Res. (M)* **1985**, 1201–1217.
44. Alberghina, G.; Bottino, F.A.; Fisichella, S.; Arnone, C. Solvent effects on the rotational barriers of the *N*,*N*-dimethylamides of 2- and 3-furoic and 2- and 3-thenoic acids. *J. Chem. Res. (S)* **1985**, 108–109.
45. Turnbull, M.M.; Nelson, D.J.; Lekouses, W.; Sarnov, M.L.; Tartarini, K.A.; Huang, T.-K. Rotational barriers in N,N-diethylbenzamides: Substituent and solvent effects. *Tetrahedron* **1990**, *46*, 6613–6622. [CrossRef]
46. Wodtke, R.; Steinberg, J.; Köckerling, M.; Löser, R.; Mamat, C. NMR-based investigations of acyl-functionalized piperazines concerning their conformational behavior in solution. *RSC Adv.* **2018**, *8*, 40921–40933. [CrossRef]
47. Friebolin, H. *Basic One- and Two-Dimensional NMR Spectroscopy*; Wiley-VCH: Weinheim, Germany, 2010; p. 319 ff.
48. Gasparro, F.P.; Kolodny, N.H. NMR determination of the rotational barrier in *N*,*N*-dimethylacetamide. A physical chemistry experiment. *J. Chem. Educ.* **1977**, *54*, 258. [CrossRef]
49. Jackman, L.M.; Cotton, F.A. (Eds.) *Dynamic Nuclear Magnetic Resonance Spectroscopy*; Academic Press: New York, NY, USA, 1975; p. 204 ff.
50. Skoglof, A.; Nilsson, I.; Gustafsson, S.; Deinum, J.; Göthe, P.O. *Cis-trans* isomerization of an angiotensin I-converting enzyme inhibitor. An enzyme kinetic and nuclear magnetic resonance study. *Biochim. Biophys. Acta* **1990**, *1041*, 22–30. [CrossRef]

51. Sheldrick, G.M. A short history of SHELX. *Acta Cryst. A* **2008**, *64*, 112–122. [CrossRef]
52. Sheldrick, G.M. *SHELXL 2014/2*; University of Göttingen: Göttingen, Germany, 2014.

Disclaimer/Publisher's Note: The statements, opinions and data contained in all publications are solely those of the individual author(s) and contributor(s) and not of MDPI and/or the editor(s). MDPI and/or the editor(s) disclaim responsibility for any injury to people or property resulting from any ideas, methods, instructions or products referred to in the content.